19th Brazilian Congress of Thermal Sciences and Engineering
November 06th-10th, 2022, Bento Gonçalves - RS - Brazil

ENC-2022-0569
AERODYNAMIC HEATING CALCULATION FOR A HYPERSONIC AIRBREATHING PROPULSION SYSTEM AT MACH NUMBER 7

Felipe Jean da Costa
Gustavo Jean da Costa
BRENG Engenharia e Tecnologia LTDA, Parque Tecnológico de São José dos Campos, Avenida Doutor Altino Bondesan, 500, Distrito de Eugênio de Melo - CEP - 12247-016 São José dos Campos, SP – Brasil
felipejean@brengtrein.com.br
gustavojean@brengtrein.com.br

Alana Aíres da Rocha Brito
ITA - Instituto Tecnológico de Aeronáutica, Praça Marechal Eduardo Gomes, nº 50 Vila das Acácias CEP. 12.228-900 São José dos Campos, SP - Brasil
alanarb21@gmail.com

Abstract. *The Hypersonic Airbreathing Propulsion System, designed at the Brazilian Aerospace Startup BRENG Engineering and Technology, is a technological demonstrator endowed with Scramjet Engine to fly in the Earth's atmosphere near 30 km altitude at speeds corresponding to the Mach number 7.Considering the high speed flight regime, the originated shockwaves and the viscous forces yield the phenomenon called aerodynamic heating under the aerospace vehicle airframe, causing the friction between the fluid filaments and the body or compression at the stagnation regions of the leading edge that converts the kinetic energy into heat within a thin layer of air which blankets the body. The temperature inside this mentioned layer increases with the square of the speed and is concentrated in the boundary-layer, where heat will flow readily from the boundary-layer to the hypersonic aerospace vehicle structure. Fay and Riddell and Eckert methods are applied to evaluate at the stagnation point and over the flat plate segments for the model, in order to calculate the aerodynamic heating allowing to determine the thermal field over the model's surface from the leading edge to the trailing edge of the proposed Hypersonic Airbreathing Propulsion System for Mach number 7 condition.*

Keywords: *Aerodynamic heating, hypersonic airbreathing propulsion, Scramjet*

1. INTRODUCTION

The Brazilian Aerospace Startup BRENG Engineering and Technology, is studying Hypersonic Airbreathing Propulsion (HAP) Systems as integrating part of INCT-PRO-HYPER (National Institute of Science and Technology in HAP) efforts, a research network involving universities, research centers, companies and headed by the Institute for Advanced Studies (IEAv) from the Brazilian Air Force. Also, BRENG is a player in the PROCAD DEFESA academic cooperation, headed by IEAv, to collaborate with the Human Resources training in HAP areas aiming the space access. The HAP system studied by BRENG, named Vector Hypersonic Vehicle (VHV), is based on the supersonic combustion (scramjet) and a laser propulsion combined cycle, such as suggested by Costa (2018). The VHV (Fig. 1) is a technological demonstrator designed to demonstrate, during the hypersonic flight speed corresponding to Mach number 7 through the Earth's atmosphere at 30 km altitude, three innovative technologies: i) waverider technology, to obtain lift from conical shock wave during the supersonic or hypersonic flight; ii) scramjet engine that consists in a hypersonic airbreathing propulsion system based on supersonic combustion, using hydrogen as fuel, and iii) laser propulsion concept, where the air breakdown phenomenon promotes the aerospace vehicle thrust and accelerates it up to supersonic/hypersonic conditions.During the hypersonic flight the scramjet engine promotes the compression and deceleration of freestream at the inlet station of the scramjet, throughout the oblique/conical shock waves. The scramjet is an aeronautical engine without moving parts and integrated as part of the aerospace vehicle, in order to conditioning the air in supersonic speeds and then to burn fuel (Hydrogen) in the combustion chamber.

The main objective of the Vector vehicle development is to empower the Brazilian Company (BRENG) in the aero-thermo-structural project area of HAP system based on supersonic combustion (scramjet) to be applied in aerospace

vehicles integrated with scramjet aiming Access to Space, in accordance with INCT PRO-HYPER and PROCAD DEFESA agreements. Therefore, a simplified version of the Vector vehicle will be presented in this manuscript, namely the scramjet engine, considering power on with Hydrogen.

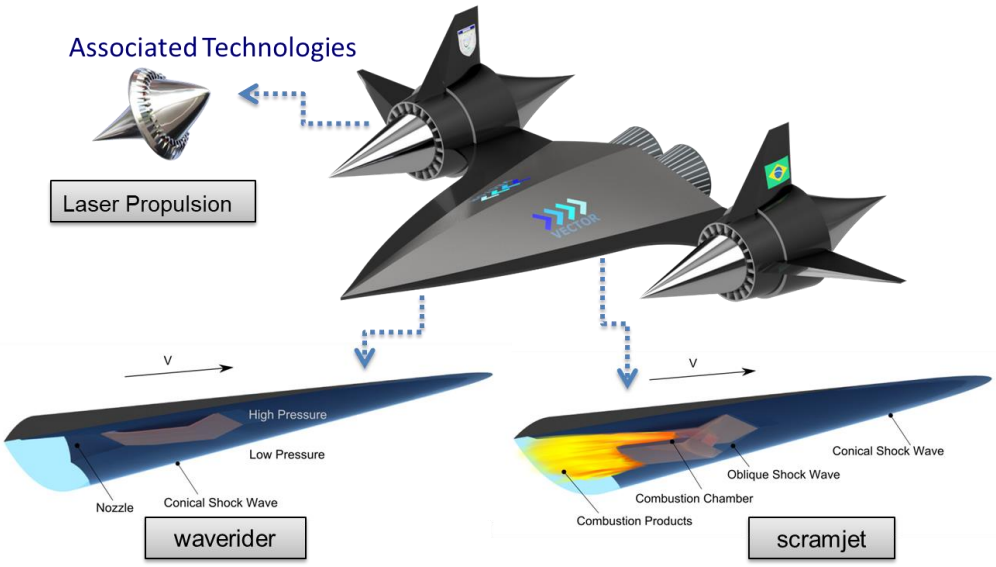

Figure 1. The Vector Hypersonic Aerospace Vehicle with waverider, scramjet and laser propulsion concepts.

2. AERODYNAMIC HEATING CALCULATION

When the air reaches supersonic/hypersonic conditions, the shock waves and the viscous forces in the boundary layer, established over a vehicle body, are responsible to decelerate the air and it yields the phenomenon called aerodynamic heating. In this case, occurs a friction between the fluid filaments and the body or the compression at the stagnation regions of leading edge that convert the kinetic energy into heat within a thin layer of air which blankets the body, where the temperature in this layer increases with the square of the speed of the vehicle, and this high temperature is concentrated in the boundary-layer, where heat will flow readily from the boundary-layer to the vehicle's surface (van Driest, 1956).

The aerodynamic heating is affected by a possible dissociation and ionization of the air that occurs at finite rates, and implies that the thermochemical equilibrium cannot be achieved in the flow field (Fay and Riddell, 1958), because there is a high static temperature in the shock layer. Furthermore, the atoms and ions release a high specific energy, if they are diffused on the surface and consequently recombined at the wall, which causes a significantly increase in the heat transferred by conventional molecular conduction. Using a non-catalytic surface will be possible to eliminate the fraction of heat transfer that is transported by atomic diffusion into the wall followed by recombination at the surface. Although, to an effective use of a non-catalytic surface, the atoms cannot recombine firstly in the gas before reaching the wall. If the wall is catalytic, the concentration of atom is reduced to the equilibrium value of the wall temperature. If the atoms recombine in the boundary layer or at the wall there will be no major effect on convective heat transfer (Fay and Riddell, 1958).

For the aerodynamic heating are applied two theories, the Fay and Riddell theory to the stagnation point due the existence of a blunted nose formed at the vehicle's leading edge during the manufacturing process; and the Eckert's reference enthalpy theory applied to the vehicle's surface assuming the air flow in the conical surfaces as a flow over a flat plate (Costa, 2016).

In terms of thermo-structural challenges, typically the extreme thermal loads on the leading edges of the vehicle have a significant magnitude in terms of heat flux, where the heat flux increases inversely to square root of the nose radius, as stagnation heat transfer theory, develop by Fay and Riddell (1958). The heat flux as function of the nose radius can be seen in the Figure 2(a), where for 1-inch (25.4 mm) nose radius, the heat flux is approximately 500 Btu/ft2-sec (5674.47 kW/m²). For a large leading-edge radius, one may obtain a lower heat flux, but several airbreathing vehicles require a small nose radius and therefore, the heat flux is significantly high (Glass, 2008). Figure 2(b) shows the aerodynamic heating for the ballistic and l g reentry vehicles, respectively (Hankey, 1988). In the ballistic reentry trajectory, one may observe an extreme heat flux, about 10,000 (Btu/ft2 s) (113,489,317 W/m²) for a short time period (20s). In other hand, the heat flux for the lifting reentry vehicle is 1% of the ballistic reentry vehicle, around 100 (Btu/ft2 s) (1,134,893.17 W/m²), but with a longer time period. Therefore, it is necessary keep in mind what type of the trajectory will be used to demonstrated any new hypersonic aerospace vehicle.

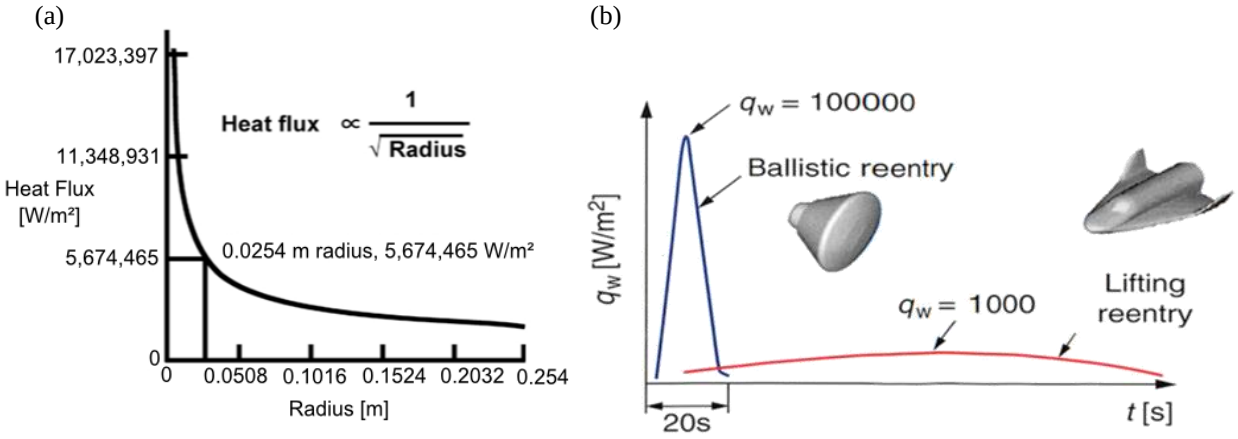

Figure 2. (a) Heat flux function of the nose radius, adapted from Glass (2008); (b) Ballistic and lifting reentry heat flux function of the trajectory, adapted from Hankey (1988).

Figure 3 shows the thermal levels encountered during a hypersonic flight by an aerospace vehicle using HAP. Note that, the heat flux (aerodynamic heating) at the nose is approximately 5000 Btu/ft²-sec (56744.7 kW/m²), at the control surface leading edge is approximately 500 Btu/ft²-sec (5674.47 kW/m²) and at the cowl leading edge is approximately 50000 Btu/ft²-sec (567447 kW/m²), respectively, due to the shock-shock interaction. Observe that, the maximum heat flux at the wing leading edge of the Space Shuttle Orbiter, is approximately 70 Btu/ft²-sec (794 kW/m²) (Glass, 2008), about one order magnitude lower than the control surface leading edge of the hypersonic aerospace vehicle using airbreathing propulsion system

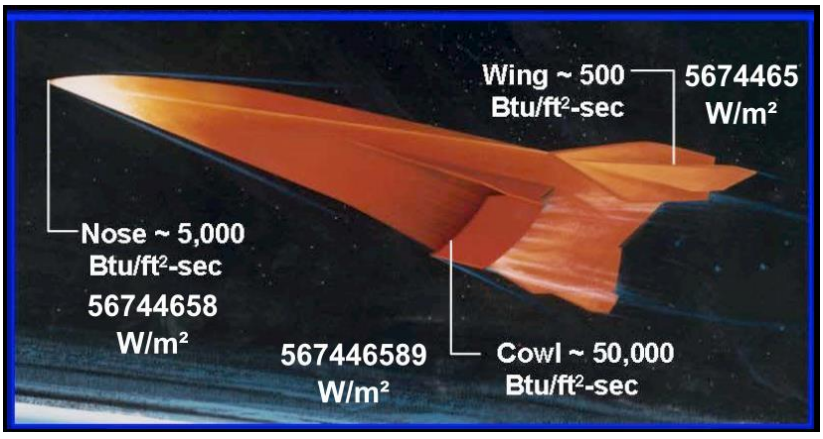

Figure 3. Thermal levels of the Hypersonic Aerospace Vehicle with HAP, adapted from Glass (2008).

2.1 Fay and Riddell Aerodynamic Heating Theory Applied to the Stagnation Point

The theory of stagnation point heat transfer in dissociated air developed by Fay and Riddell considers the effects of diffusion and of atom recombination in the boundary layer. The boundary-layer equations, at the stagnation point, can be reduced exactly to a set of nonlinear ordinary differential equations (self-similar boundary-layer equations) even when the chemical reactions proceed so slowly that the boundary layer not achieve the thermochemical equilibrium. They considered the energy transport through a motionless dissociated gas with temperature and concentration gradients.

The convective heat flux at the stagnation point may be given by:

$$\dot{q}_w = \left[\frac{k}{\bar{c}_p}\frac{\partial h}{\partial y}\right]_w + \left[\sum\left(\frac{k}{\bar{c}_p}\right)\left(h_i - h_i^0\right)\left\{\left(L_i - 1\right)\left(\frac{\partial c_i}{\partial y}\right) + \left(\frac{L_i^T c_i}{T}\right)\left(\frac{\partial T}{\partial y}\right)\right\}\right]_w \tag{1}$$

where, k, $\bar{c}_p$, h, T are thermal conductivity, specific heat per unit mass at constant pressure considering translation, rotation and vibration, enthalpy per unit of mass of mixture, absolute temperature, respectively. The subscript w

indicates the condition on the wall. c_i is mass fraction of component i. L_i and L_i^T are the Lewis number and thermal Lewis number, respectively, given by $L_i = D_i \frac{\rho \bar{c}_p}{k}$ and $L_i^T = D_i^T \frac{\rho \bar{c}_p}{k}$, where D_i and D_i^T are diffusion coefficient and thermal diffusion coefficient, respectively.

Fay and Riddell present the following similarity, which includes the usual Howarth and Mangler transformations of independent variables *x* and *y*, as proposed by Lees given by:

$$\eta = \frac{r\, u_e}{\sqrt{2\,\xi}} \int_0^y \rho \, dy \tag{2}$$

$$\xi = \int_0^x \rho_w \, \mu_w \, u_e \, r_o^{2k} \, dx \tag{3}$$

Further, some dimensionless dependent variables were used for them and are given by:

$$g = \frac{h + u^2/2}{h_s} \qquad \theta = \frac{T}{T_e} \qquad s_i = \frac{c_i}{c_{ie}} \tag{4}$$

where, subscripts *e* refers to the free stream condition and *s* refers to the free stream condition at the stagnation point.

The convective heat flux at the stagnation point equation in terms of the dimensionless temperature and enthalpy distributions can be written as follow:

$$\dot{q}_w = \left[\left(2 \left(\frac{\rho}{\mu} \right)_w \left(\frac{du_e}{dx} \right)_s \right)^{1/2} \frac{k_w h_s}{c_{pw}} \right] \left[g_\eta + \sum c_{ie} \left(\frac{h_i - h_i^0}{h_s} \right) \left\{ \left(L_i - 1 \right) s_{i\eta} + L_i^T s_{i\eta} \frac{\theta_\eta}{\theta} \right\} \right]_w \tag{5}$$

where $s_{i\eta} = \frac{\partial s_i}{\partial \eta}$, $\theta_\eta = \frac{\partial \theta}{\partial \eta}$, and $g_\eta = \frac{\partial g}{\partial \eta}$, respectively. Also ρ, μ, $\left(\frac{du_e}{dx} \right)_s$ are the density, dynamic viscosity, and the velocity gradient at the stagnation point, respectively.

Therefore, the heat transfer at the stagnation point in dissociated air presented by Fay and Riddell is given by:

$$\dot{q}_w = \frac{0.763}{(\mathrm{Pr}_w)^{0.6}} (\rho_e \mu_e)^{0.4} (\rho_w \mu_w)^{0.1} \left[(h_o)_e - h_w \right] \left[1 + \left(Le^{0.52} - 1 \right) \frac{h_d}{(h_o)_e} \right] \left[\left(\frac{du_e}{dx} \right)_t \right]^{0.5} \tag{6}$$

where, the velocity gradient $\left(\frac{du_e}{dx} \right)_s$ may be defined using the Newtonian modified theory for the stagnation point, and is given by

$$\left(\frac{du_e}{dx} \right)_s = \frac{1}{R_N} \sqrt{\frac{2\left(p_e - p_\infty \right)}{\rho_e}} \tag{7}$$

where, R_N is the nose radius, p_e, ρ_e, p_∞, are the pressure and density outside of the boundary layer, and pressure at the freestream, respectively.

2.2 Eckert's Reference Enthalpy Theory

In the literature we can found several methods to calculate the heat transfer and skin friction in high-speed boundary layers (Nielsen, 1955), remarkably the mean-enthalpy method to laminar boundary layers used by Rubesin and Johnson (1949), that was applied to turbulent boundary layers by Sommer and Short (1955). Subsequently, Eckert developed the reference enthalpy method assuming that the global effects of the boundary layer with varying properties can be replaced by the boundary layer with constant properties, that corresponds to average properties or at the reference enthalpy (or temperature), which can be found a priori (Heiser and Pratt, 1995).

The convective heat flux for thermal boundary layer with variable properties can be given by the product of the conductance (Stanton number) and an enthalpy difference, as shown by the following equation:

$$q_w = St \cdot \rho_e V_e (h_{aw} - h_w) \tag{8}$$

where, ρ_e and V_e are the density and velocity of the gas in adjacent inviscid flow outside the boundary layer, respectively. haw and h_w correspond to the adiabatic wall enthalpy and wall enthalpy, respectively. The Stanton number *(St)*, for laminar flow, corresponds to a dimensionless coefficient given by

$$St = \frac{0.332}{\mathrm{Pr}^{3/2}\mathrm{Re}^{1/2}} \tag{9}$$

where, *Pr* and *Re* are Prandtl number and Reynolds number, respectively.

Considering the perfect gas assumption, we may replace the adiabatic wall enthalpy and wall enthalpy, h_{aw} and h_w by:

$$h = c_p \cdot T \tag{10}$$

Therefore, the adiabatic wall temperature may be calculated by the following equation:

$$T_{aw} = T_e \cdot [1 + r \cdot \frac{\gamma - 1}{2} \cdot M_e^2] \tag{11}$$

where the recovery factor *r*, is the ratio of the adiabatic wall enthalpy and total enthalpy related by the kinetic energy. Due to finite thermal conductivity for real gas, part of the thermal energy is conducted away from the higher temperature region of the wall to the gas at low temperature, thus lowering the h_{aw}, and the recovery factor is given by

$$r = \frac{h_{aw} - h_e}{\frac{2}{V_e}} \tag{12}$$

For laminar and turbulent flows, the recovery factor r may be obtained by:

$$r = \begin{pmatrix} \sqrt{\mathrm{Pr}} & \textit{for laminar} \\ \sqrt[3]{\mathrm{Pr}} & \textit{for turbulent} \end{pmatrix} \quad \textit{where} \quad \mathrm{Pr} = \frac{\mu \, c_p}{k} \tag{13}$$

Therefore, the convective heat flux for thermal boundary layer with variable properties can be given by

$$q_w = \frac{0.332}{\mathrm{Pr}^{3/2}\mathrm{Re}^{1/2}} \cdot \rho_e V_e \ (h_{aw} - h_w) \tag{14}$$

Assuming perfect gas the convective heat flux for thermal boundary layer with variable properties can be given by

$$q_w = \frac{0.332}{\mathrm{Pr}^{3/2}\mathrm{Re}^{1/2}} \cdot \frac{\rho_e V_e}{c_p} \ (T_{aw} - T_w) \tag{15}$$

Considering the Eckert's reference enthalpy method, the reference temperature T^* is given by

$$T^* = T_e + 0.5(T_w - T_e) + 0.22r(T_s - T_e) \tag{16}$$

where, T_e is the flow temperature after the normal shock wave and T_w is the wall temperature, and the stagnation temperature (T_s) is calculated by:

$$T_S = T_e[1+\frac{\gamma-1}{2}\cdot M_e^2] \quad (17)$$

where, M_e is the Mach number after the normal shock wave.

The recovery facto r, shown in Eq. 13, is calculated from the Prandtl number valuated at T^*.

To obtain the T^*, firstly the stagnation temperature from Eq. 17 need to be calculated and assume a value for T^*, then calculate Pr^* through Eq. 13. By Sutherland's law (Eq. 18) the reference dynamic viscosity (μ^*) is given, the reference thermal conductivity (k^*), given by Eq. 19, is estimated, and using the software HAP (Hypersonic Airbreathing Propulsion) the reference specific heat at constant pressure (c_p^*) is computed. The recovery factor is obtained from Eq. 13 and then used to calculate the reference temperature (T^*) from Eq. 16. Once obtained the new T^*, the new Pr^* is calculated through Eq. 13 and then a second T^* using the same Eq. 16. Repeat the whole process until the T^* results converge.

$$\mu^* = 1.46\ 10^{-6}\left(\frac{T^{*1.5}}{T^*+111}\right) \quad (18)$$

$$k^* = 1.993\ 10^{-6}\left(\frac{T^{*1.5}}{T^*+112}\right) \quad (19)$$

Once the reference temperature T^* has been computed, it is possible to proceed to calculate the heat transfer given by:

$$q_w = \frac{0.332\,\rho_e u_e\ \ (h_{aw}-h_w)}{\mathrm{Pr}^{3/2}\,\mathrm{Re}_x^{1/2}} \quad (20)$$

The enthalpy at the adiabatic wall (h_{aw}) is calculated by:

$$h_{aw} = h_e + r\frac{u_e^2}{2} \quad (21)$$

where, u_e is the flow velocity and h_e is the flow enthalpy, given by:

$$h_e = c_p T_e \quad (22)$$

where, c_p is the specific heat at constant pressure and T_e is the flow temperature after the normal shock.

Similarly, to the flow enthalpy, the enthalpy at the wall (h_w) is calculated utilizing:

$$h_w = c_p T_w \quad (23)$$

where, T_w is the wall temperature.

The reference Reynolds number (R_e^*) is given by:

$$\mathrm{Re}_{xx}^* = \frac{\rho^* u_e x}{\mu^*} \quad (24)$$

where, u_e is the flow velocity and x is the surface extension. The reference density (ρ^*) is given by the perfect gas relation, i.e.,

$$\rho^* = \frac{p_2}{RT^*} \quad (25)$$

where, p_2 is the flow pressure, R is the air gas constant and T^* is the reference temperature and the μ^* is the reference dynamic viscosity, which can be calculated from Eq. 18.

After the calculation of all variables presented above it is possible to obtain the heat transfer rate over the surface by the Eckert's reference temperature methodology given by Equation 16.

2.3 Scramjet Inlet and Combustor Power on

The aerodynamic design of the scramjet inlet (with one compression ramp) and combustor was performed considering freestream conditions on design point assuming at the inlet: two-dimensional adiabatic flow, calorically perfect gas; inviscid flow; shock-on-lip and shock-on-corner conditions. In the combustor we considered fuel injection; chemical equilibrium; constant area assumption; and viscous effects were taken into account through the skin friction coefficient. In Fig. 4 the constant area combustor schematics is shown, where the cowl leading edge position corresponds to the intersection point of the horizontal line that limits the area of air capture b_0, at the design point, and the shockwave originated at the compression ramp leading edge, establishing the shock-on-lip condition in order to prevent flow spillage. The end position of the compression ramp is determined through its intersection with the reflected shockwave originated in the cowl leading edge. It is emphasized that the isolator station is neglected, and the combustor entry is located immediately after the compression ramp. In Fig. 4, the station 1 (x_1, y_1) is the end of the external compression, θ and β correspond to the compression ramp and shockwave angles, respectively. The reflected oblique shockwave angle is given by β_R. The coordinates x_3 and x_4 correspond to the compression ramp length and the total length of the scramjet engine (the distance between the compression ramp leading edge and the end of the combustor), respectively.

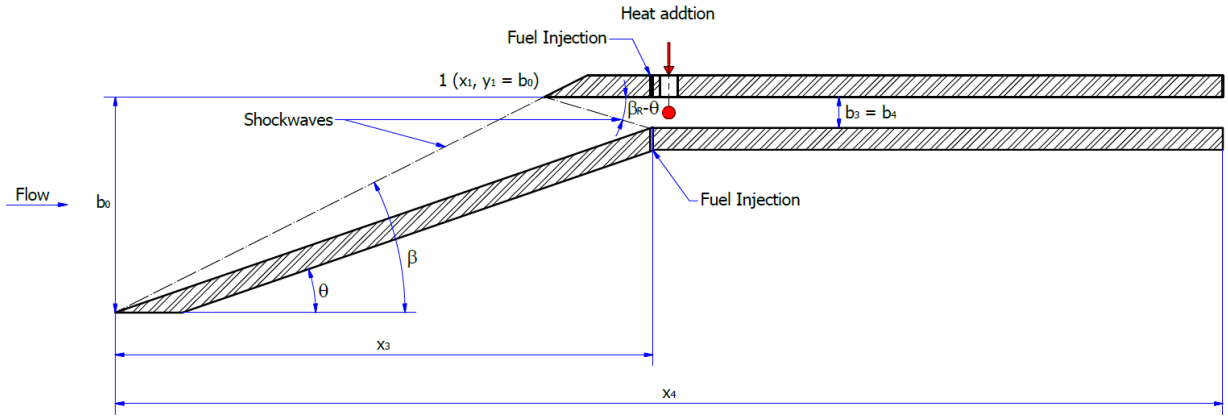

Figure 4. scramjet dimensioning for constant area (Costa et al., 2017).

The conservation equations were applied to the control volume showed in Fig. 5 with the assumptions: steady and quasi-one-dimensional flow, chemical equilibrium, and neglecting the effects of gravitational, acceleration, electrical, and magnetic fields on the motion or energy of the fluid. For mass conservation we have:

$$\dot{m}_3 + \dot{m}_f = \dot{m}_4 \tag{26}$$

For momentum conservation in the axial direction:

$$p_3 A_3 + \dot{m}_3 u_3 + \dot{m}_f u_f + F_x = p_4 A_3 + \dot{m}_4 u_4 \tag{27}$$

For energy conservation:

$$\dot{m}_3 \left(h_3 + \frac{u_3^2}{2} \right) + \dot{m}_f \left(h_f + \frac{u_f^2}{2} + \frac{v_f^2}{2} \right) + \dot{W} + \dot{Q} = \dot{m}_4 \left(h_4 + \frac{u_4^2}{2} \right) \tag{28}$$

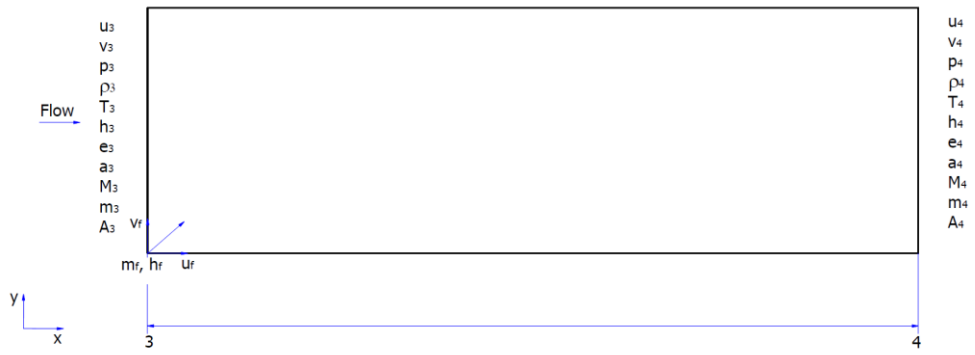

Figure 5. Combustor control volume for constant area (Costa et al., 2017).

3. RESULTS AND DISCUSSIONS

Considering the air in chemical equilibrium, the thermodynamic properties over the scramjet engine regions from 0-4 (Figure 6) will assume different values of that encountered by calorically perfect gas approach, due the temperatures higher than 400K cause a change in thermodynamic parameters such as the specific heat at constant pressure c_p and the ratio of specific heats γ. In this way, using the air equilibrium module of the in-house code developed we can obtain the property distribution along of scramjet engine.

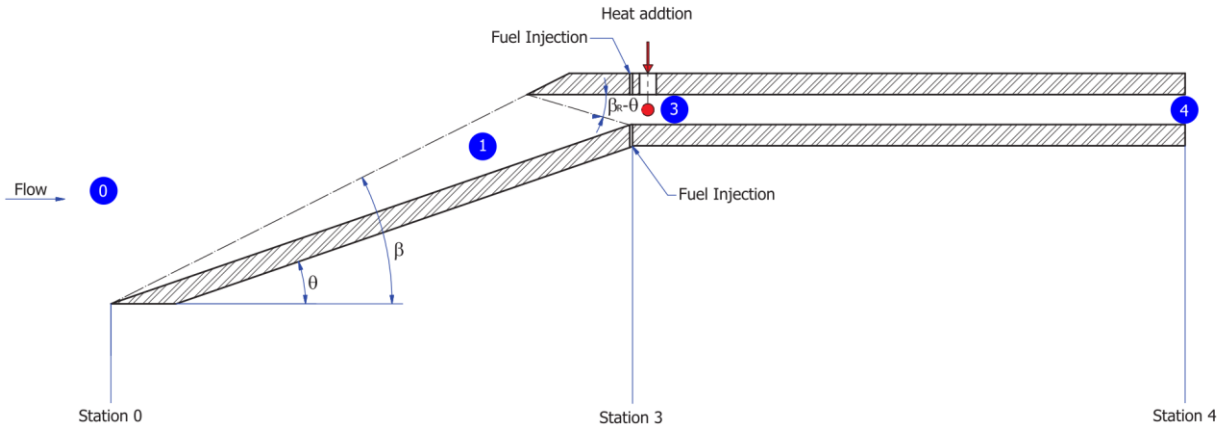

Figure 6. VHV scramjet regions (0-4) for Analytical Theoretical Analysis.

First of all, the atmospheric thermodynamic properties at the altitude of interest (at 30 km altitude) and the problem given data need to be known (Table 1).

The Property distribution assuming air in chemical equilibrium for the Vector scramjet engine at 30 km altitude and speed corresponding to Mach 7 is summarized in Table 2, following the named regions presented by Fig. 6.

Table 1. Thermodynamic air properties at 30 km of altitude and problem given data

PROBLEM GIVEN DATA		**AIR PROPERTIES AT 30 Km ALTITUDE**	
Ramp Nose Radius	0.005 m	Speed of Sound	301.7 m/s
Cowl Nose Radius	0.002 m	Temperature	226.5 K
Altitude	30 Km	Density	$1.84\ 10^{-2}$ kg/m³
Wall Temperature	300 K	Pressure	1,197 Pa
γ	1.4		
R	287		
Mach Number (M_1)	7		
Speed at Mach 7	2,111.9 m/s		

Table 2. Heat Flux at Stagnation Point of the Ramp and Cowl Leading Edges

Region	p [Pa]	T [K]	Mach
1	13,053.54	628.70	3.80
3	59,978.19	1,071.29	2.53
4	243,883.79	2,339.42	1.01

Applying Fay and Riddell theory at the stagnation point where the nose radius of the vehicle is 0.002 m, and considering the mission profile at 30 km of altitude and Mach number 7, the heat flux at stagnation point can be obtained as show in the Table 3.

Table 3. Heat Flux at Stagnation Point of the Ramp and Cowl Leading Edges

Radius [m]	Heat flux [W/m²]
0.002	3,461,726.62

The heat flux in the lower, upper, scramjet compression and expansion ramps, and scramjet fins (side wall) is provided by Eckert's reference enthalpy theory. To aerodynamic heating is needed to take in account the Reynolds number for each station presented in the Fig. 6. This procedure assumes instantaneous heat transfer to the vehicle structure, which provides a higher heat flux. This situation represents a conservative assumption, because not occurs in real world.

Solving the equations 13, 17, 18, 19, 24 and 25 by iteration, and considering the air in chemical equilibrium it is possible to obtain the reference temperature T^* by equation 16 and hence the parameters as Prandtl number, recovery factor, Reynolds number, density and c_p could be computed for each station presented in Fig.6. Finally, based on the reference temperature and parameters mentioned above, the heat flux per region (Fig. 6) are presented in the Tables 3 to 4. Table 4 is summarized at Fig. 7.

Table 4. Heat flux over the Vector scramjet engine regions

Mach	q_1 [W/m²]	q_3 [W/m²]	q_4 [W/m²]
7	72,326.55	100,953.10	38,155.12

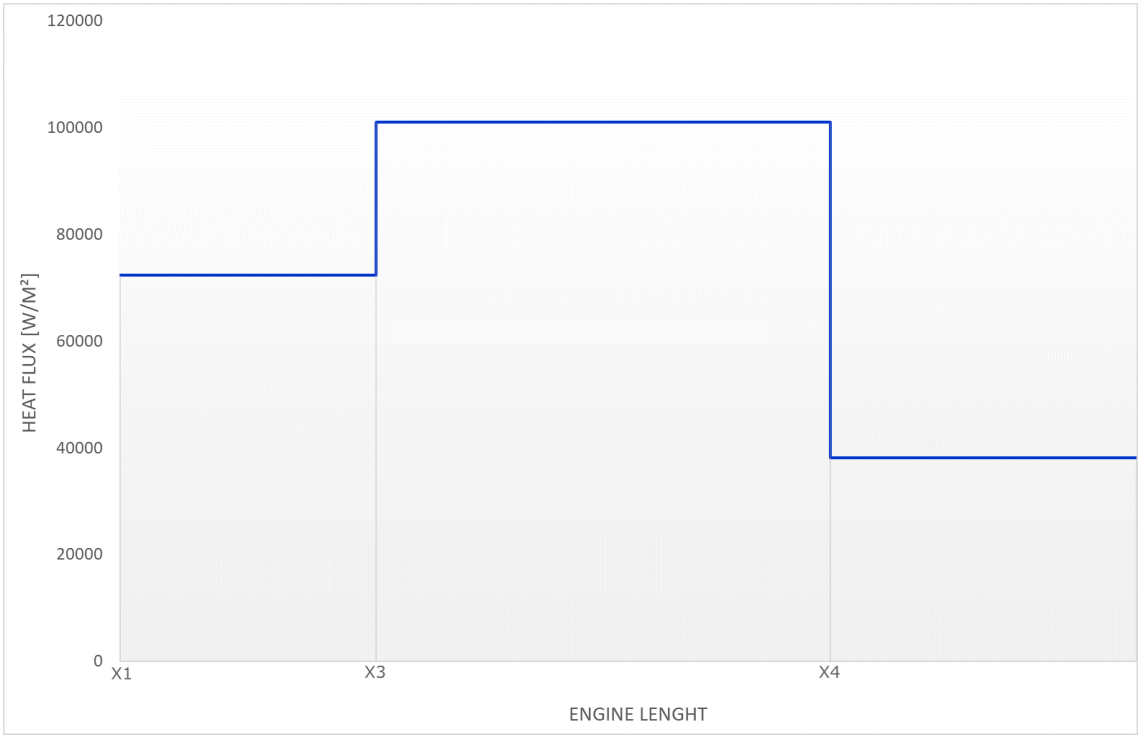

Figure 7. VHV Heat flux over the Vector scramjet engine regions.

4. CONCLUSIONS

Hypersonic flight introduces extreme thermal loads on the leading edges of the vehicle, which generates high temperature around the vehicle surfaces. Consequently, high temperature materials and high temperature coatings should be employed. The extreme thermal loads on the leading edges of the scramjet engine have a significant magnitude in terms of heat flux. The heat flux increases inversely to square root of the nose radius, as mentioned before, as stagnation heat transfer theory, developed by Fay and Riddell. For a large leading-edge radius, one may obtain a lower heat flux, but several airbreathing vehicles require a small nose radius and therefore, the heat flux is significantly high. The aerodynamic heating at the stagnation point for the VHV considered a minimum nose radius, to not disturb hardly the shockwave structure. The Eckert's Reference Enthalpy theory provided the aerodynamic heating over the surfaces of the VHV scramjet engine, which the results are in perfect compliance with the studied literature. Further works should be conducted for the mechanical design, thermos-structural analysis, and the correct material selection and thermal protection system.

5. ACKNOWLEDGEMENTS

The first author would like to express his gratitude to INCT PRO-HYPER (INCT - MCTI/CNPq/CAPES/FAPs n. 16/2014), CAPES PROCAD/DEFESA n.15/2019, and to São José dos Campos Technological Park (PqTec).

6. REFERENCES

Costa, F.J., 2014. Thermo-Structural Analysis of the Brazilian 14-X Hypersonic Aerospace Vehicle. Master thesis, Instituto Tecnológico de Aeronáutica, São José dos Campos, Brazil.

Costa, F.J., Rolim, T.C., Rêgo, I.S., Minucci, M.A.S., Oliveira, A.C., and Toro, P.G.P. Aerodynamic Heating of the Brazilian 14-X Hypersonic Waverider Scramjet Vehicle at Mach Numbers 7 And 10. In: 16th Brazilian Congress of Thermal Sciences and Engineering. November 07-10th, 2016, Vitória, ES, Brazil.

Driest, E.R.,1956. The Problem of Aerodinamic Heating. Aeronautical Engineering Review, p 26-41.

Eckert, E.R.G., April, 1954. Survey on Heat Transfer at High Speeds. WADC Technical Report, p 54-70.

Fay, J.A. and Riddell, F.R., 1958. Theory of Stagnation Point Heat Transfer in Dissociated Air. Journal of The Aeronautical Sciences.

Glass, D.E. Ceramic Matrix Composite (CMC) Thermal Protection Systems (TPS) and Hot Structures for Hypersonic Vehicles. In: 15th AIAA International Space Planes and Hypersonic Systems and Technologies Conference, 28 April - 1 May 2008 (AIAA 2008-2682), Dayton, Ohio – USA.

Hankey, W.L. Re-Entry Aerodynamics. AIAA Education Series, J.S. Przemieniecki, Series Editor-in-Chief, 1988, AIAA, ISBN 978-0-930403-33-1

Heiser, W.H. and Pratt, D.T., 1995. Hypersonic Air breathing Propulsion. - Wright Patterson Air Force Base, Ohio, 1st Edition.

Nielsen, J.N., 1960. Missiles Aerodynamics. McGraw-Hill Book, New York, 1st Edition.

Lees, L., 1956. Laminar Heat Transfer Over Blunt-Nosed Bodies at Hypersonic Flight Speeds. Jet propulsion. Vol.26, n. 4, p 259-274

Rubesin, M.W. and Johnson, H.A., 1949. A Critical Review of Skin-friction and Heat-transfer Solutions of the Laminar Boundary Layer of a Flat Plate. Tans. ASME, vol. 71, n. 4, pp. 385-388.

Sommer, S.C. and Short, B.J., Mach, 1955. Free-flight Measurements of Turbulent Boundary-layer Skin Friction in the Presence of Severe Aerodynamic Heating at Mach Numbers from 2.8 to 7.0. NACA Tech. Notes 3391.

7. RESPONSIBILITY NOTICE

The authors are the only responsible for the printed material included in this paper.